Biomedical Microdevices (2022) 24: 14
https://doi.org/10.1007/s10544-022-00614-2

Glucose sensing on screen-printed electrochemical electrodes based on porous graphene aerogel @prussian blue

Tao Hu[1] · Di Wang[1] · Jian Xu[1] · Ke Chen[1] · Xiao Li[1] · Hong Yi[1] · Zhonghua Ni[1]

Accepted: 1 February 2022 / Published online: 26 February 2022

Abstract

As one of the three major chronic diseases, diabetes often causes many complications, which can affect various parts of the body and even threaten the life of the patients. At present, the situation of diabetes in the world is quite serious. Accurate detection of blood glucose is very important for the diagnosis, treatment and medication of diabetes as well as the self-management of diabetic patients. In this paper, an electrochemical glucose biosensor was developed based on screen-printed electrode (SPE) modified with composite material of graphene aerogel (GA) and Prussian blue (PB) (denoted as GA@PB), which was fabricated via chemical reduction using L-ascorbic acid as a reducing agent through a freeze-drying process. Glucose was specifically captured by glucose oxidase (GOx) which were immobilized into the GA@PB by chitosan. The structure and performance of the sensor were characterized by scanning electron microscopy (SEM), Raman spectroscopy measurements, Fourier transform infrared spectrometer (FTIR), cyclic voltammetry (CV) and amperometric detection. The sensor exhibited a linear range of 0.5–6.0 mmol·L^{-1} with limit of detection (LOD) of 0.15 mmol·L^{-1}, indicating that the combination of graphene aerogel and Prussian blue possess well conductivity and catalytic performance.

Keywords Glucose · Graphene aerogel · Prussian blue · Screen-printed electrodes · Electrochemical detection

Abbreviations

SPE	Screen-printed electrode
PB	Prussian blue
GA	Graphene aerogel
GOx	Glucose oxidase
CV	Cyclic voltammetry

1 Introduction

Diabetes is one of the fastest growing health challenges in the twenty-first century, and the number of adults living with diabetes has more than tripled over the past 20 years. Diabetes and a series of serious complications caused by diabetes are endangering 463 million adults and the number will rise to 700 million by 2045 (Yuen et al. 2019). At present, it is still difficult to cure diabetes completely, so patients should take long-term treatment to maintain normal blood glucose level, which means that frequent and accurate blood glucose detection is becoming a widespread demand. Automatic biochemical analyzer and blood glucose meter are usually applied to clinical blood glucose detection. However, the reliance on expensive instrument and complex operation hardly meets the needs of patients for accurate, sensitive, reliable and inexpensive daily glucose detection. Therefore, a series of glucose biosensors have been developed rapidly because of their advantages including convenience, low-cost and miniaturization (Yoo and Lee 2017). Among them, electrochemical technique has attracted much attention and stand out as a promising and widely used technique because of its rapid response, good selectivity, simple operation, wide linear range and low limit of detection (Toh et al. 2014; Bansod et al. 2017). Boronic acid incorporated on conducting polymer (Brownlee et al. 2018) or gold nanoparticle (Wang et al. 2018) electrodes was utilized to improve performance of electrode by changing the equilibrium potential. Later on, nanostructures such as nanoparticles (Dayakar et al. 2017),

✉ Xiao Li
lx2016@seu.edu.cn

✉ Hong Yi
yihong@seu.edu.cn

✉ Zhonghua Ni
nzh2003@seu.edu.cn

Tao Hu
hutao@seu.edu.cn

[1] School of Mechanical Engineering, and Jiangsu Key Laboratory for Design and Manufacture of Micro–Nano Biomedical Instruments, Southeast University, Nanjing 211189, China

nanowires (Liu et al. 2017), nanoporous particles (Xie et al. 2017) were introduced for glucose detection because of the large specific surface area of nanomaterials, together with the enhanced catalytic effects and conductivity.

Ferric ferrocyanide, known as Prussian blue (PB) has been widely used due to its magnetic, electrochromic and electrochemical properties (Xu et al. 2017). PB is considered as ''artificial enzyme peroxidase'' due to its high activity and good selectivity towards the reduction of hydrogen peroxide (Farah et al. 2012; Karyakin and Karyakina 2001; Ding et al. 2008), which has been applied to enzyme-free hydrogen peroxide sensor as substitute of catalase enzyme sensor. PB can reduce hydrogen peroxide at a rapid rate with low over-potential, which reduces the interference current caused by the reaction of the remaining substances, improving the accuracy of detection. However, the poor conductivity of PB limits its further use on electrochemical sensors (Chen et al. 2012). In this condition, the combination of PB and nanomaterials offers a positive solution (Li et al. 2007; Zhai et al. 2009). Graphene, one of the hottest and most promising two-dimensional nanomaterials, is widely used as a substrate material on electrochemical electrodes due to its high conductivity, large surface area, great stability and other unexpected properties (Chen et al. 2012; Zhang and Choi 2015; Inagaki and Kang 2014; Pumera 2013). Additionally, 3D porous graphene aerogel inheriting most advantages of graphene with larger surface area and complex pore structure shows remarkable capacity and bonding ability to other particles (Xu et al. 2016; Zhou et al. 2017). Consequently, the combination of PB and graphene aerogel preforms superior conductivity, high activity, selectivity towards the reduction of hydrogen peroxide which is the iconic product of glucose oxidation. Previously, 3D porous graphene aerogel has been synthesized and embedded in microfluidic chip by our group to realize blood glucose detection, while the sensitivity was still need to be improved (Xu et al. 2020). Therefore, the introduce of PB and the combination with 3D graphene aerogel may improve the performance of our former glucose biosensor, which deserves further investigation.

Screen-printed technology was applied to print electrodes on substrate using conductive ink to form a small chip, easily realizing mass production with low variance with the advantage of flexibility, small structure and low cost (Sljukic et al. 2006; Grennan et al. 2001). Among them, flexible substrates exhibit the potential to be applied to portable and wearable devices, especially in point of care (POC) test. Herein, CTS/GOx-GA@PB modified screen-printed electrode (SPE) was fabricated to act as a flexible and portable glucose sensor. Briefly, GA@PB was directly synthesized on the working electrode of SPE by freeze-drying the hydrogel of graphene and PB precursor mixture, followed by immobilizing glucose oxidase (GOx) to the graphene aerogel (GA) which obtained in the previous step with the assistance of chitosan (CTS). Glucose captured on graphene aerogel was catalytically oxidized by glucose oxidase to produce hydrogen peroxide, and hydrogen was specifically reduced by PB. The use of porous graphene aerogel could increase the conductivity and sensitivity due to the large specific surface area, greatly amplifying the reduction current. Results showed good selectivity and stability of the as-fabricated glucose sensor with a low limit of detection (0.15 mM) and a wide linear range (0.5–6 mM), which supported the speculation that combining PB particles with graphene aerogel could improve the sensitivity and broaden the application field of porous graphene aerogel in bio-sensing.

2 Material and methods

2.1 Materials and apparatus

All chemicals were analytical grade. Graphene oxide (GO) solution was purchased from Chenfeng Technology (Changzhou, China). Acetic acid and $FeCl_3 \cdot 6H_2O$ were purchased from Sinopharm Chemical Reagent Co., Ltd (Shanghai, China). $K_3Fe(CN)_6$ was purchased from Maclean (Shanghai, China). Glucose oxidase (GOx), fructose, maltose, sucrose and lactose were purchased from Aladdin (Shanghai, China). Chitosan, Uric acid (UA) and glucose were purchased from Sigma-Aldrich (St. Louis, USA). L-ascorbic acid (LA) was purchased from Alfa Aesar (Shanghai, China) and silver conductive paint was purchased from Mechanic (Hong Kong, China). A phosphate buffer solution (PBS), 10 mM, was employed in this work.

Polyethylene terephthalate (PET) polyester film was purchased from Shanghai Texiang Electrical Insulation Material Company (Shanghai, China). Conductive carbon ink, silver ink, silver/silver chloride ink and insulation ink were purchased from Guangzhou Youte New Material Company (Guangzhou, China).

Scanning electron microscopy (SEM, Helio NanolabTM 600i, FEI Company, America) and Raman spectroscopy measurements (Alpha 300 Raman-AFM, Witec, Germany) were used to observe the morphology of the proposed GA@PB composite material. Fourier Transform Infrared Spectrometer (FTIR, Nicolet iS10, Thermo Fisher, America) was used to analyze the composition of the sample.

All of the electrochemical experiments were conducted on the electrochemical workstation (CHI660E, Chenhua, Shanghai, China). The proposed sensor owned a three-electrode configuration containing a working electrode of the CTS/GOx-GA@PB modified conductive carbon layer, a reference electrode of Ag/AgCl layer and a counter electrode of conductive carbon layer.

Fabrication of the screen-printed electrode.

As it is shown in Supplementary Fig. S1A, the screen-printed electrode (SPE) consists of three layers. The bottom layer is silver ink, which mainly plays a conductive role. At the same time, the silver (Ag) layer has three pins for connection to the electrochemical workstation. The middle layer is composed of conductive carbon ink and silver/silver chloride (Ag/AgCl) ink. The silver/silver chloride ink is used as the reference electrode (RE). As for the conductive carbon ink, the arc-shaped portion serves as the counter electrode (CE), and the central circular portion serves as the working electrode (WE) for active materials deposition and enzyme immobilization. The uppermost layer is insulation ink, which mainly plays the role of insulation protection. The dimensions of SPE can be seen in Fig. S1B.

SPE was prepared by a screen-printing machine (SPC-3050, Shenzhen Kejing Zhida, China) and four screen-printing plates were designed corresponding to four ink layers (Fig. S2). Figure 1A illustrates the preparation process and size of SPE. Firstly, Ag ink was printed on the clean PET substrate. Secondly, conductive carbon ink was printed to serve as CE and WE. Thirdly, Ag/AgCl ink was printed to serve as RE. Finally, insulation ink was printed. After each printing step, the printed layer was cured at 80 °C for half an hour to dry the ink. Figure 1B presents the prepared SPE as the substrate of biosensor. The SPE was rinsed using ultrapure water before further use.

2.2 *In situ* preparation of GA@PB and immobilization of GOx

GA@PB was prepared via a freeze-drying technology using LA as the reducing agent. The *in situ* synthesis steps of GA@PB with mass ratio of PB to graphene 1:1 were as follows: 0.3 g LA and 0.0266 g $FeCl_3 \cdot 6H_2O$ were dissolved in 3.5 mL of ultrapure water and sonicated to form evenly solution A. 0.049 g $K_3Fe(CN)_6$ was dissolved in 1 mL of ultrapure water and magnetically stirred for 10 min. The above solution was mixed with 3 mL GO solution (10 mg/mL) and magnetically stirred for half an hour to form solution B. Solution A was mixed with solution B and magnetically stirred for 10 min to form the target mixture. A thin layer of conductive silver paste was evenly covered on the circular working electrode area of SPE to enhance the adhesion of GA@PB to SPE. 20 µL of the above mixture was evenly dropped onto the silver paste, then SPE was heated in water bath at 40 °C for 16 h. After that, SPE was kept in the refrigerator at -20 °C for 48 h and then was freeze-dried to obtain GA@PB modified SPE.

Chitosan was used to immobilize GOx. At first, 15 µL of GOx (50 mg/mL) was evenly added dropwise to the surface of GA@PB modified working electrode and was allowed to dry in its natural state. Then, 15 µL of 0.5% chitosan in 3% acetic acid was drop-casted on the surface, and the SPE was stored at 4 °C for at least 12 h. The proposed screen-printed glucose sensor based on CTS/GOx-GA@PB was finally prepared.

2.3 H_2O_2 and glucose detection

Cyclic voltammetry measurements were used to detect H_2O_2 to verify the sensing principle. It was conducted in 20 ml PBS solution containing H_2O_2 at a sweep rate of 50 mV/s, with the potential range of -0.5 V to 0.5 V. Amperometric detection measurements were used to obtain the calibration curve of the sensor detecting H_2O_2 and glucose, respectively. For H_2O_2 detection, the working area of the sensor was immersed in 20 mL of PBS, and H_2O_2 was added

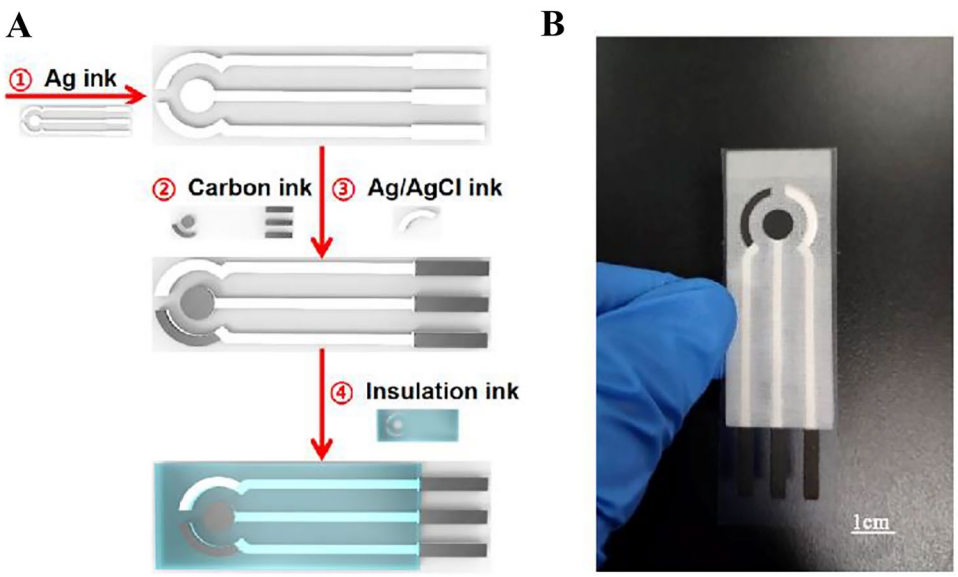

Fig. 1 (**A**)The process for preparing SPE. (**B**) The image of the prepared SPE

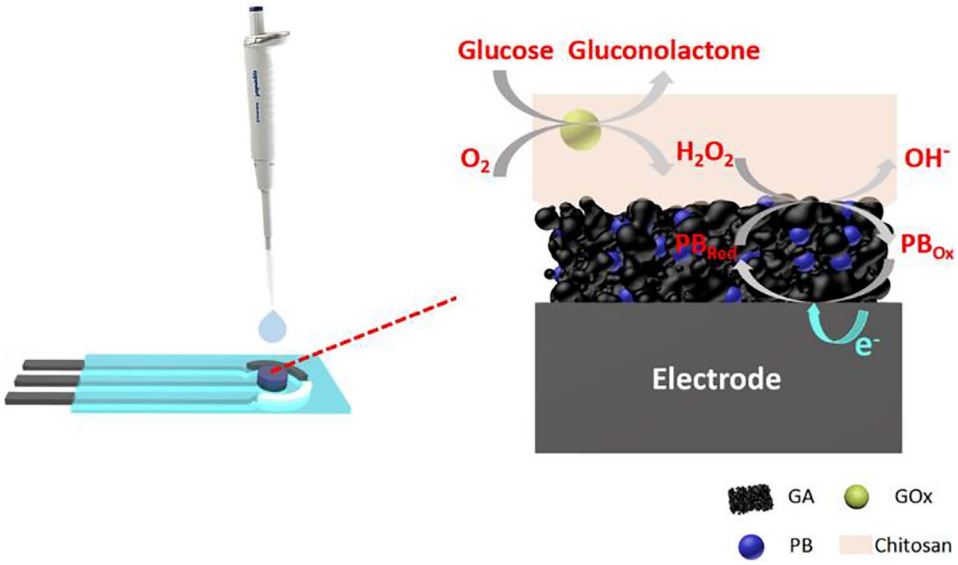

Scheme 1 Schematic illustration of electrochemical glucose detection using the proposed CTS/GOx-GA@PB based screen-printed sensor

dropwise to the solution every once in a while, and current was recorded under corresponding test potential. For glucose detection, glucose was dissolved into PBS to produce glucose solution samples with concentrations ranging from 0.5 to 7.5 mM. Then, 300 µL of PBS was dropped directly to the working area of the sensor and current was recorded at a potential of -0.35 V, and 300 µL of PBS containing glucose was dropped to the working area after PBS solution was aspirated away with a pipette. The sensor was incubated for 9 min and current was then recorded at the same potential. All of the detection and tests were repeated three times independently at room temperature and the error bars were calculated from these three independent measurements.

3 Results and discussion

3.1 Validation of the sensing principle

Scheme 1 explains the mechanism of glucose detection with our proposed biosensor. When glucose is dropped on the working area of the sensor, it is catalytically oxidized by GOx immobilized by chitosan on the GA@PB electrode into gluconolactone and H_2O_2. PB with satisfactory electrocatalytic activity for H_2O_2, further boosted the sensitivity of proposed biosensor to detect H_2O_2 and glucose. Briefly, H_2O_2 is reduced to OH^- by the reduced-state PB, and the reduced-state PB changes to its oxidized state simultaneously. Then PB in the oxidized state obtains electrons from the electrode and changes back to its reduced state, which will lead to the change of system current. The mechanism for H_2O_2 electrocatalytic reduction by PB and the electron transfer between PB and electrode can be described by Eqs. 1 and 2 according to the literature (Oliver et al. 2013). In addition, the use of chitosan simplified the immobilization of GOx without introducing other substances for activation. Consequently, the glucose concentration can be determined by detecting its product H_2O_2 according to the change of system current.

$$K_4Fe_4^{II}[Fe_{II}(CN)_6]_3 + 2H_2O_2 \rightarrow Fe_4^{III}[Fe_{II}(CN)_6]_3 + 4OH^- + 4K^+ \quad (1)$$

$$Fe_4^{III}[Fe^{II}(CN)_6]_3 + 4e^- + 4K^+ \rightarrow K_4Fe_4^{II}[Fe^{II}(CN)_6]_3 \quad (2)$$

Accordingly, in order to verify the sensing principle of the proposed biosensor, detection of H_2O_2 with the proposed sensor was firstly conducted through cyclic voltammetry (CV). In order to confirm the positive effect of PB to H_2O_2 detection, two sensors were investigated for comparative experiments, with pure GA and GA@PB decorated the working electrode, respectively. Figure S3 presents the CV curves of the SPE of the working area modified with pure GA in PBS with the presence and absence of H_2O_2. The cathode reduction current peak of the CV curves increased with the increasing of H_2O_2 concentration, which indicated that H_2O_2 was reduced during this process due to the electrocatalytic ability of graphene. For comparison, the comparative experiment was performed using GA@PB modified SPE, and the result shows the similar trend. The comparison of two sensors' CV tests is shown in Fig. S4. Obviously, for the same concentration of H_2O_2, the current response of SPE based on GA@PB was higher than that of SPE based on pure GA, which manifested that the introduction of PB improved the sensitivity of the sensor to detect H_2O_2.

3.2 Characterization of GA@PB

GA@PB was obtained by freeze-drying process, which was prepared by *in situ* chemical reduction using LA as the reducing agent. As a conductive support of PB, 3D porous GA not

only improves the stability of PB, but also exhibited large specific surface area, which was beneficial to charge transfer in electrochemical detection. GA@PB composites were characterized by SEM, Raman spectroscopy and FTIR. Figure 2A and B display the SEM images of GA@PB in different magnifications. Compared to the SEM image of GA (Fig. S5), it can be found that a lot of PB nanoparticles are attached to the 3D GA in Fig. 2A and B shows that PB nanoparticles still existed inside the pores of GA, manifesting the 3D porous structure of GA@PB. In addition, the rough surface and porous structure confirmed that the 3D porous graphene structure was still maintained under the condition of PB introduction, further proving the feasibility of this preparation method. The Raman spectroscopy of GA and GA@PB was shown in Fig. 2C. Both Raman spectra of GA@PB and pure GA showed two typical peak bands D and G, locating at 1350 cm^{-1} and 1580 cm^{-1} assigned to graphene (Su et al. 2018; Shao et al. 2011). The intensity ratio of D to G can qualitatively reflect the defect density of carbon materials (Hu et al. 2018; Meng et al. 2018). The D/G intensity ratio of GA@PB was comparable to that of pure GA, indicating little changes occurred for GA structure when PB was introduced. Figure 2D shows the FTIR spectra of GA and GA@PB. The peak at 1750 cm^{-1} and 1270 cm^{-1} corresponded to the C=O and C-O bond of carboxyl groups in GA. Compared with GA, an absorption band at 2070 cm^{-1} appeared in the FTIR spectrum of GA@PB, which was attributed to C-N stretching absorption band in the Fe^{2+}-CN-Fe^{3+} of PB (Gangola et al. 2014; Ma et al. 2014). Other weak peaks in the spectra corresponded to the C=C bond and C–O–C bond of graphene. All these characterization results indicated the successful preparation of GA@PB composites.

3.3 Optimization of the biosensor

Amperometric detection experiments were conducted in order to verify that this biosensor could be used to detect H_2O_2 quantitatively. At first, the detection potential of H_2O_2 reduction was optimized to gain better current response. The working area of GA@PB based sensor was immersed in 20 mL of PBS electrolyte and a certain potential was applied to the system. Then 2 mM H_2O_2 was dropwise added to the solution and amperometric response of this system was recorded. As a result, the cathodic reduction current peak appeared at around -0.35 V in Fig. S4, so the detection potentials were further selected at -0.3 V, -0.35 V and -0.4 V, respectively. As shown in Fig. 3A, the current change achieved maximum at -0.35 V, so -0.35 V was determined as the optimal detection potential of GA@PB based sensor.

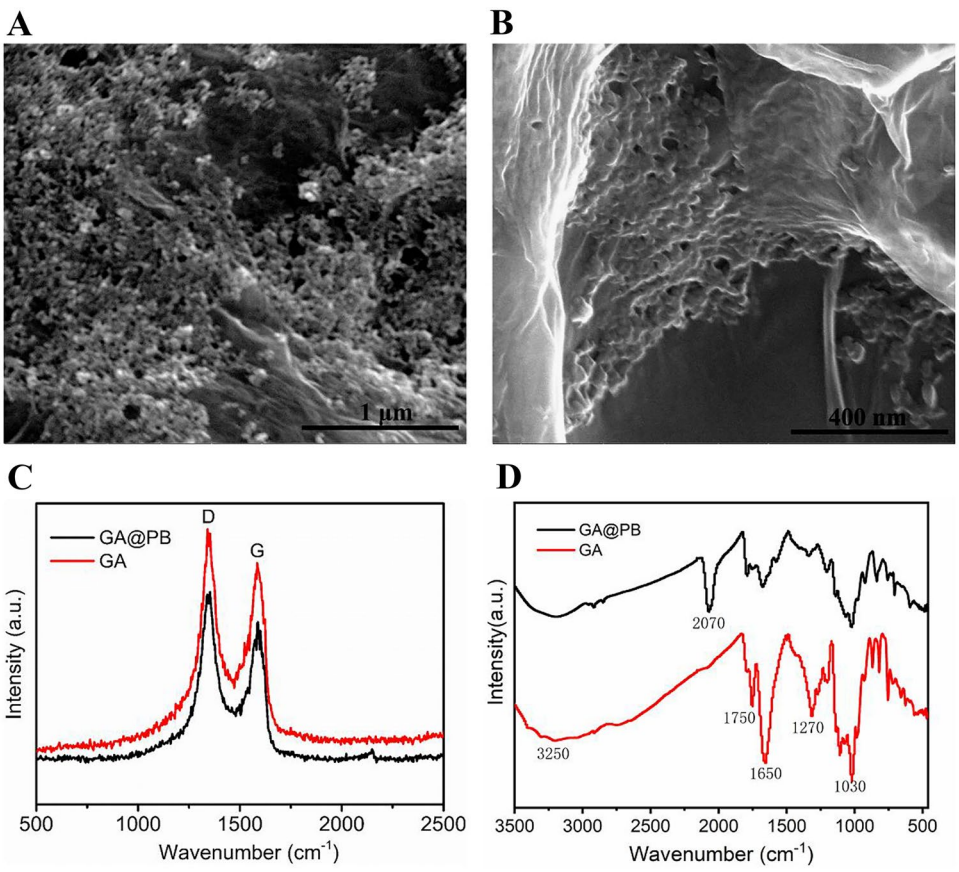

Fig. 2 SEM images of GA@PB at (**A**) low magnification and (**B**) high magnification. (**C**) Raman spectroscopy of GA and GA@PB. (**D**) FTIR spectra of GA and GA@PB

In addition, the ratio of PB to GA was an important factor needed to be considered, because the proper ratio can maintain the balance between good conductive and efficient catalytic sites of H_2O_2. Under the optimal potential of -0.35 V, the GA@PB modified SPE with different ratios (PB:GA = 0.25, 0.5 and 1) were immersed in PBS solution containing 2 mM H_2O_2. In Fig. 3B, as the proportion of PB increased, the current response improved apparently and achieved maximum at the ratio of 0.5. With the proportion of PB increased further, the current response decreased, which might result from the inferior conductivity caused by lower GA ratio. As a result, the ratio of 0.5 was chosen as the optimal proportion.

As for the detection of glucose, it was mainly determined by detecting H_2O_2, which is the product of catalytic oxidation of glucose by GOx. However, a very important factor in the detection was the incubation time after glucose solution was dropped on the sensor. Although the process of the oxidation of glucose by GOx was fast, we founded that keeping glucose in contact with the enzyme for a long time could enhance the current, which indicated the incomplete reaction of glucose. This phenomenon may be presumed that chitosan encapsulated glucose oxidase and hindered the rapid reaction. Therefore, the incubation time was further explored. The incubation time was optimized using amperometric at -0.35 V when 5 mM glucose solution was dropped on the sensor. As shown in Fig. 3C, after 3 mM glucose solution was dropped on sensor, the system current response increased with the increasing incubation time and stabilized at 9 min. The current change difference between 9 and 11 min could be ignored, so 9 min was chosen as the optimal incubation time.

3.4 Amperometric detection of glucose

Our proposed enzymatic screen-printed electrochemical biosensor was used to obtain the calibration plots for glucose concentration detection by measuring different concentrations of glucose in PBS. The measurements were conducted under the optimal conditions determined in 3.3. The biosensors were firstly incubated by different concentrations of glucose for 9 min, and then they were detected with amperometric at the potential of -0.35 V, respectively. Figure 4 shows the current responses of sensors after incubation by different concentrations of glucose. The current gradually decreased as time increased, and the current showed the same trend of change in different glucose concentrations. For the convenience of calculation, we chose the average current value of 45–50 s as the current value to perform the following calculations. As it can be seen in Fig. 4B, with the glucose concentration increases, the current response decreases gradually and Fig. 4A demonstrates that $|I\text{-}I_0|$ increase linearly with glucose concentration in the range of 0.5-6 mM. Furthermore, the difference in current is linearly related with the glucose concentration as the following equation.

$$|I - I_0| = -0.30746 + 2.96847C \tag{3}$$

where, I is the current value of SPEs after incubation by glucose, I_0 is the current value of SPEs in PBS without any glucose, and C represents the glucose concentration.

A linear relationship between current difference and the glucose concentrations were obtained in the range of 0.5–6 mM ($R^2 = 0.994$) and the limit of detection (LOD) for glucose of our sensor was 0.15 mM. The LOD was calculated according to the 3S/m criterion, where m is the slope of the calibration curve and S is estimated as the standard deviation of current response in PBS without any glucose. The key performance indicators of the proposed sensor were compared to other glucose biosensors using composite nanomaterial to improve sensing performance and using electrochemical as the detection method, which was provided in Table S1. The LOD and linear range of the proposed sensor are enough to analyze the glucose in practical situations.

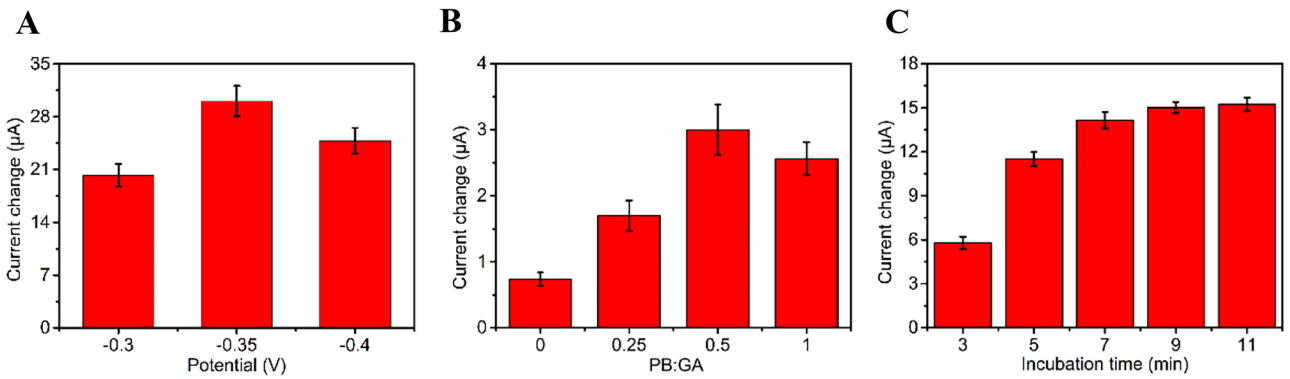

Fig. 3 (**A**) Current response of the GA@PB based sensor to 2 mM H_2O_2 under voltage conditions of -0.3 V, -0.35 V and -0.4 V, respectively. (**B**) Current response of the sensor to 2 mM H_2O_2 under conditions of different ratios of PB and GA. (**C**) Current response of the CTS/GOx-GA@PB based sensor to 5 mM glucose under different incubation times of 3 min, 5 min, 7 min, 9 min and 11 min

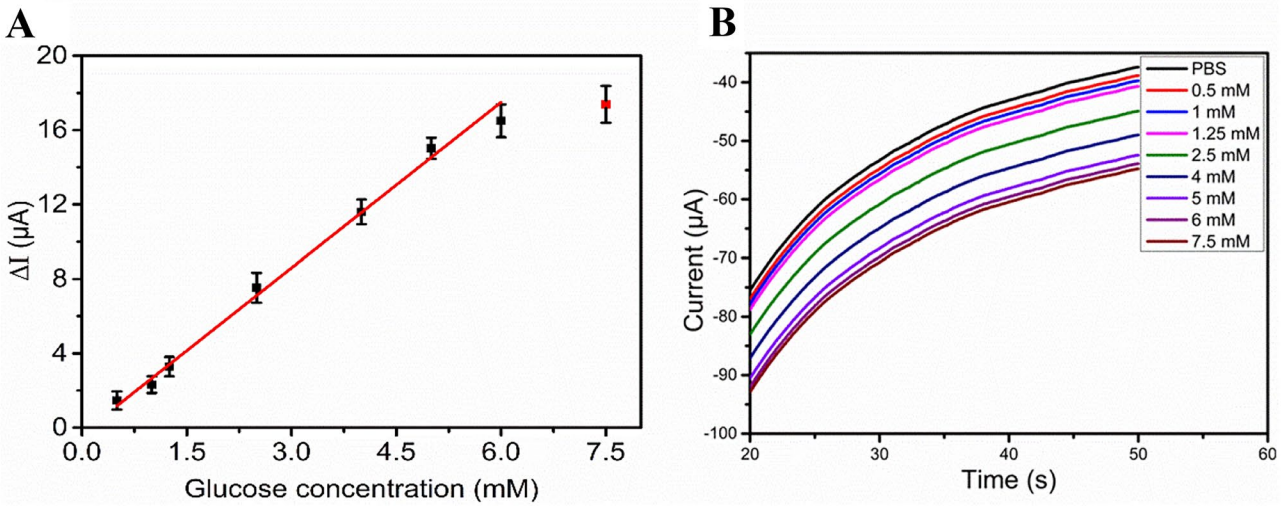

Fig. 4 (**A**) Linear plots of the proposed biosensor to different concentrations of glucose. (**B**) shows the amperometric responses upon adding different concentration glucose from 0 to 7.5 mM

3.5 Selectivity and stability of the sensor

In order to exclude the false positive caused by the interference of other substances, selectivity is a key parameter biosensor should possess. Some representative possible interferences that usually coexist with glucose in human serum were tested with the same concentration of 5 mM, including lactose, maltose, fructose, sucrose, ascorbic acid (AA) and uric acid (UA) (Meng et al. 2018). Figure 5A shows that significantly current change only occurred in the solution containing glucose in contrast with the negligible change in solution containing other interferences, concentration of which is much lower than that of glucose in actual physiological environment. Therefore, the sensor behaved good selectivity, which may result from the specific catalysis of GOx to glucose, the specific catalysis of PB to H_2O_2 as well as the low detection potential.

Stability is a key factor in evaluating the performance of biosensors as well. The sensor was stored in fridge at -20 ℃ for 5 weeks and current response to 5 mM glucose solution was tested every week. Figure 5B illustrates that current change decreased slightly over time and retained about 82%

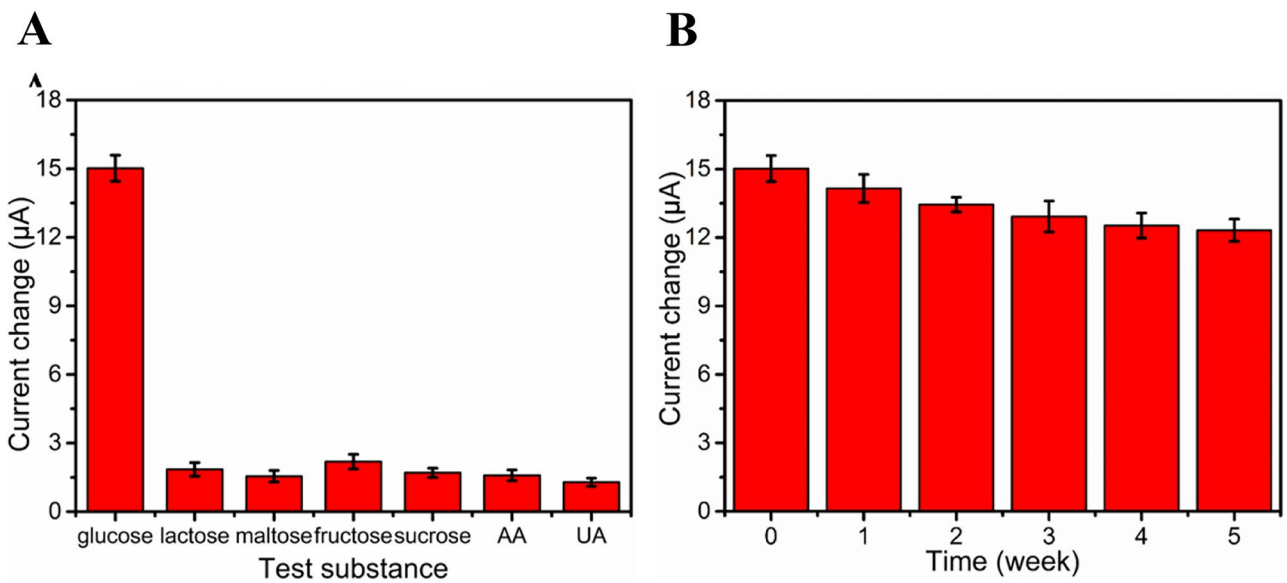

Fig. 5 (**A**) Current change of the sensor when glucose and other interfering substances are added, respectively. (**B**) Stability of sensor over 5 weeks under storage condition of -20 ℃

Table 1 Results for the determination of glucose in human serum samples

Samples	Blood glucose (mM)	Found (mM)	Recovery (%)	RSD (%) N = 3
1	6.74	6.17	91.55	6.88
2	4.75	4.88	102.66	4.89
3	5.59	6.28	112.34	9.98
4	9.5	9.88	105.05	4.26
5	10.86	11.59	106.72	5.89

of its initial response, which may be the result of inactivation of GOx. As a result, the sensor exhibited excellent long-term stability.

3.6 Real sample analysis

The sensor was further applied for the detection of glucose in real serum samples to study its practicality. The real human serum samples were firstly diluted five times with PBS. Background current (I_0) was detected by dropping 400 µL of PBS on the surface of working electrode area at -0.35 V. Then, 400 µL of diluted sample was dropped on the surface of the same area to achieve the test current (I). According to the calibration curve and current change (I-I_0), the glucose concentration of the diluted sample was calculated and real concentration of the sample was five times of this value. Compared with the standard value measured by hospital, the recovery (%) was in the range from 91.55% to 112.34% and relative standard deviation (RSD, %) was under 10% (Table 1). Therefore, the sensor showed good accuracy and precision and had considerable potential in practical glucose detection under the condition of dilution.

4 Conclusion

In this work, a low-cost, easy prepared and portable electrochemical sensor was fabricated for glucose detection. The sensor was constituted by one-step *in situ* chemical synthesis of GA@PB aerogel on the working electrode surface of SPE together with GOx immobilization into aerogel with the help of chitosan. Owing to the strong electrochemical catalytic reduction characteristics of PB for H_2O_2 and specificity of GOx, this sensor exhibited satisfactory selectivity and accuracy, with linearity range of 0.5–6.0 mmol L^{-1} and LOD of 0.15 mmol L^{-1}. Finally, the application of proposed sensor for glucose detection in human serum samples was also evaluated. Additionally, the successful combination of CTS/GOx-GA@PB and the structure of screen-printing electrode further proved that method we proposed previously for preparing GA have good universality and provided promising potential for other detection. The application of this sensor provided possibilities of simple and mass production at lower cost and flexible substrate for portable and wearable devices, which can be used in hospital, at home or even outdoors.

Supplementary Information The online version contains supplementary material available at https://doi.org/10.1007/s10544-022-00614-2.

Acknowledgements This work was supported by the National Key Scientific Instrument and Equipment Development Project (Grant No.: 51627808), National Natural Science Foundation of China (Grant No. 51605088), and Natural Science Foundation of Jiangsu Province (Grant No. BK20170667, BK20201278), the Fundamental Research Funds for the Central Universities (2242016K41022), and the Zhishan Youth Scholar Program of SEU.

Declarations

Conflicts of interest The authors declare that there is no conflict of interest.

References

B. Bansod, T. Kumar, R. Thakur, S. Rana, I. Singh, Biosens. Bioelectron. **94**, 443–455 (2017)
B.J. Brownlee, M. Bahari, J.N. Harb, J.C. Claussen, B.D. Iverson, Appl. Mater. Interfaces **10**(34), 28351–28360 (2018)
L. Chen, X.J. Wang, X.T. Zhang, H.M. Zhang, J. Mater. Chem. **22**(41), 22090–22096 (2012)
T. Dayakar, K. Venkateswara Rao, K. Bikshalu, V. Rajendar, S.H. Park, Mater. Sci. Eng. C **75**, 1472–1479 (2017)
H. Ding, L. Zhao, Y. Li, X. He, Asian J. Chem. **20**(3), 2327–2336 (2008)
A.M. Farah, F.T. Thema, E.D. Dikio, Int. J. Electrochem. Sci. **7**(6), 5069–5083 (2012)
M.P. Gangola, S. Jaiswal, Y.P. Khedikar, R.N. Chibbar, Food Chem. **154**, 127–133 (2014)
K. Grennan, A.J. Killard, M.R. Smyth, Electroanalysis **13**(8–9), 745–750 (2001)
T. Hu, Y. Ye, K. Chen, F.F. Long, W. Sang, Y.L. Zhou, D.K. Sun, Z.H. Ni, Anal. Methods **10**(48), 5749–5754 (2018)
M. Inagaki, F.Y. Kang, J. Mater. Chem. A **2**(33), 13193–13206 (2014)
A.A. Karyakin, E.E. Karyakina, Russ. Chem. Bull. **50**(10), 1811–1817 (2001)
Z.F. Li, J.H. Chen, W. Li, K. Chen, L.H. Nie, S.Z. Yao, J. Electroanal. Chem. **603**(1), 59–66 (2007)
X. Liu, W. Yang, L. Chen, J. Jia, Electrochim. Acta **235**, 519–526 (2017)
J. Ma, X.F. Hou, B. Zhang, Y.N. Wang, L.C. He, J. Pharm. Biomed. Anal. **91**, 24–31 (2014)
W. Meng, Y.Y. Wen, L. Dai, Z.X. He, L. Wang, Sens. Actuators, B Chem. **260**, 852–860 (2018)
J.D. Oliver, M. Gaborieau, E.F. Hilder, P. Castignolles, J. Chromatogr. A **1291**, 179–186 (2013)
M. Pumera, Electrochem. Commun. **36**, 14–18 (2013)
M. Shao, X. Xu, J. Han, J. Zhao, W. Shi, X. Kong, M. Wei, D.G. Evans et al., Langmuir **27**(13), 8233–8240 (2011)
B. Sljukic, N.A. Malakhova, K.Z. Brainina, C.E. Banks, R.G. Compton, Electroanalysis **18**(9), 928–930 (2006)
S. Su, Z.W. Lu, J. Li, Q. Hao, W. Liu, C.F. Zhu, X.Z. Shen, J.Y. Shi et al., New J. Chem. **42**(9), 6750–6755 (2018)

S.Y. Toh, K.S. Loh, S.K. Kamarudin, W.R.W. Daud, Chem. Eng. J. **251**, 422–434 (2014)
L. Wang, W. Zhu, W. Lu, X. Qin, X. Xu, Biosens. Bioelectron. **111**, 41–46 (2018)
W.-Q. Xie, Y.-X. Gong, K.-X. Yu, J. Chromatogr. A **1520**, 143–146 (2017)
X. Xu, F.W. Ming, J.Q. Hong, Y.Q. Xie, Z.C. Wang, Mater. Lett. **179**, 52–56 (2016)
Y. Xu, S. Zheng, H. Tang, X. Guo, H. Xue, H. Pang, Energy Storage Mater. **9**, 11–30 (2017)
J. Xu, K. Xu, Y. Han, D. Wang, X. Li, T. Hu, H. Yi, Z. Ni, Analyst (2020)
E.H. Yoo, S.Y. Lee, Sensors (Basel) **10**(5), 4558–76 (2017)
L. Yuen, P. Saeedi, M. Riaz, S. Karuranga, H. Divakar, N. Levitt, X. Yang, D. Simmons, Diabetes Res. Clin. Pract. **157** (2019)
J.F. Zhai, Y.M. Zhai, D. Wen, S.J. Dong, Electroanalysis **21**(20), 2207–2212 (2009)
W.L. Zhang, H.J. Choi, J. Intell. Mater. Syst. Struct. **26**(14), 1826–1835 (2015)
L.N. Zhou, Z.B. Yang, J. Yang, Y.G. Wu, D.S. Wei, Chem. Phys. Lett. **677**, 7–12 (2017)